Percolating networks and liquid–liquid transitions in supercooled water

2006 J. Phys.: Condens. Matter 18 S2247

(http://iopscience.iop.org/0953-8984/18/36/S02)

INSTITUTE OF PHYSICS PUBLISHING JOURNAL OF PHYSICS: CONDENSED MATTER

J. Phys.: Condens. Matter **18** (2006) S2247–S2259 doi:10.1088/0953-8984/18/36/S02

Percolating networks and liquid–liquid transitions in supercooled water

Alla Oleinikova and Ivan Brovchenko

Physical Chemistry, University of Dortmund, 44221 Dortmund, Germany

E-mail: alla@pc2a.chemie.uni-dortmund.de and brov@heineken.chemie.uni-dortmund.de

Received 30 January 2006
Published 24 August 2006
Online at stacks.iop.org/JPhysCM/18/S2247

Abstract

The anomalous behaviour of various properties of liquid water upon cooling may be explained by approaching the percolation transition of the four-coordinated water molecules or by approaching the liquid–liquid transition. We have found these two explanations are intrinsically closely related by locating the line of the percolation transitions of the four-coordinated water molecules with respect to the liquid–vapour and liquid–liquid transitions of ST2 water. The saturated liquid water upon cooling crosses the percolation threshold of the four-coordinated water molecules, which is close to the binodal (spinodal) of the first (lowest-density) liquid–liquid transition of water. This finding agrees with the known close relation between the phase transition and the percolation transition of physical clusters. The lowest-density amorphous water phase is characterized by presence of a percolating network of the four-coordinated water molecules. The line of the percolation transitions of tetrahedrally ordered water molecules (with arbitrary coordination number) envelops the whole region where liquid–liquid transitions occur. So, the percolating network of the tetrahedrally ordered water molecules is absent in the highest-density amorphous water phase.

1. Introduction

The density maximum of saturated liquid water as well as the anomalous behaviour of some properties of liquid water were qualitatively explained a long time ago by assuming the existence of the two kinds of water molecules with different local order (see [1] for historical review). In particular, liquid water was considered as a mixture of 'ice-like' component and 'normal' liquid. Such 'ice-like' species possess a lower entropy and lower density than 'normal' water molecules. Upon cooling, the fraction of the 'ice-like' species increases, providing a liquid density maximum at some temperature. This simple *mixture model of liquid water*, first proposed by Whiting in 1884 [2], was essentially developed in subsequent studies, and numerous modifications of the mixture model of water can be found in the literature now.

The experimental finding of a singular-like behaviour of some properties of liquid water [3] at about 228 K [4] renewed discussions of a possible origin of the anomalous water properties. In 1979, Stanley attributed this singular temperature to the *percolation transition* of the four-coordinated water molecules [5], which are rather similar to the 'ice-like' species in the first mixture model of water. It was shown that the connectivity of species with definite number NN of the neighbours in the first coordination shell is far from random [5]. In particular, the species with NN = 4 have higher probability to have similar neighbours in the first coordination shell, that results in the formation of extended patches of four-coordinated water molecules. With increasing population, four-coordinated water molecules can form an infinite network via correlated-site percolation transition [5]. As the local density of the patches of the four-coordinated water molecules differs from the density of the rest of the fluid, an increase of their clustering gives rise to an increase of density fluctuations, which may be responsible for the thermodynamic anomalies observed experimentally [6, 7]. Computer simulations of liquid water evidence the existence of an infinite hydrogen-bonded network [8], which includes clusters of spatially correlated patches of the four-coordinated molecules [9–11]. Varying the definition of connectivity between two water molecules, a correlated-site percolation transition of four-coordinated water molecules was confirmed to be consistent with ordinary random-bond percolation in a three-dimensional lattice [12].

Anomalous behaviour of supercooled water may also be attributed to the existence of a liquid–liquid phase transition of supercooled water. This idea appeared due to the experimental observation of the phase transition between low-density (LDA) and high-density (HDA) amorphous ices [13] and got further support from various experimental and simulation studies (see [14] for a recent review). The discovery of the third form of amorphous ice, very-high-density amorphous ice (VHDA) [15], was followed by the observation of multiple liquid–liquid transitions in computer simulations of various water models [16–18]. Finally, the multiplicity of the phase transitions between various amorphous water phases was confirmed by experimental observation of the two-step transformation LDA $\rightarrow$ HDA $\rightarrow$ VHDA upon pressurization [19].

Depending on the mutual location of the liquid–vapour and liquid–liquid transitions, two main scenarios are possible. If some liquid–liquid phase transition meets the liquid–vapour transition at a triple point, thermodynamic properties of liquid water should diverge approaching the spinodal of the liquid–liquid transition [16, 17, 20–22]. In the absence of a triple point, anomalous behaviour of liquid water may be the result of a distant effect of one [20, 21, 23–26] or several [16–18] liquid–liquid critical points, which are shifted with respect to the liquid branch of the liquid–vapour coexistence curve in pressure and temperature. The smooth transition between these two scenarios may be achieved by tuning parameters of the system [17, 20, 21, 23, 24, 27]. In particular, in the modified van der Waals model [20], the liquid–liquid critical point shifts from negative to positive pressures with strengthening of the hydrogen bonds. A similar trend is observed in the ST2 water model due to the account of the long-range Coulombic interactions [17, 25, 28].

Anomalous behaviour of liquid water may be seen in the models which do not show liquid–liquid transition [29]. However, even in this singularity-free scenario, anomalous properties of liquid water may be attributed to the distant effect of the *hidden* liquid–liquid transition, which occurs in water with modified molecular parameters [21, 23, 27]. The effect of a hidden liquid–liquid phase transition is well known for aqueous solutions with a closed-loop phase diagram. In particular, the closed-loop phase diagrams of aqueous solutions of some pyridines shrink and disappear due to the substitution of heavy water by normal water [30]. Variation of the molecular parameters (deuteration of water) has the same effect on the closed-loop phase diagram as variation of pressure. Liquid–liquid transition in the mixtures of pyridines with normal water appears with increasing [31] or decreasing [32] pressure. The hidden phase

transition causes an increase of density (concentration) fluctuations in solutions which do not show liquid–liquid phase separation [33]. On the other hand, the liquid–liquid transitions may not necessarily result in liquid density anomalies [34, 35].

Phase transition is closely related to the percolation transition of physical clusters [36]. In particular, line of percolation transition meets the coexistence curve at the critical point. At sub-critical temperatures, percolation of physical clusters may be expected close to the spinodal curve, which cannot be defined unambiguously, however, in the case of short-range inter-particle interaction [37]. The line of the percolation transitions of the hydrogen-bonded water clusters in aqueous solution was observed close to the liquid–liquid coexistence curve [38]. Due to so close a relation between percolation and phase transition, two explanations of the anomalous water properties, one based on the idea of the percolation of the four-coordinated molecules, and another based on the existence of a liquid–liquid transition, may just represent different views of the same physical phenomenon.

To clarify the relation between percolation transition, anomalous properties of liquid water and liquid–liquid transitions in supercooled water, we have located lines of the percolation transitions of the four-coordinated molecules and tetrahedrally ordered molecules with respect to the liquid–vapour and liquid–liquid phase transitions of the ST2 model of water.

2. Model system and simulation methods

The phase diagram of the ST2 water model [39] was obtained in [16, 17] by direct simulations of the coexisting phases in the Gibbs ensemble [40] and by simulations of isotherms in the NPT ensemble with restricted density fluctuations [41, 42]. This water model shows the closest correspondence with the experimentally observed transitions between various amorphous ices [19, 43]. There are three liquid–liquid phase transitions of ST2 water in the supercooled region. The corresponding four phases of the supercooled ST2 water may be attributed to the experimentally observed LDA, normal-density water, HDA, and VHDA [43]. The lowest-density liquid–liquid phase transition has the critical point at negative pressure and crosses the liquid–vapour coexistence curve at a triple point at about 270 K, whereas the liquid density maximum is located at about 310 K.

We have analysed the clustering and percolation of water molecules, which possess some specific local order. Two main parameters of the local order were used: the number NN of the neighbours in the first coordination shell and the tetrahedricity measure θ. A water molecule belongs to the first coordination shell of the reference molecule if the distance between the two oxygen atoms does not exceed 3.5 Å. To characterize the tetrahedral arrangement of arbitrary chosen water molecule, we used the tetrahedricity measure θ [44]:

$$\theta = \frac{6\Sigma_{j\neq i}\left(l_i - l_j\right)^2}{15\Sigma_i l_i^2}, \tag{1}$$

where l_i are the lengths of the six edges of the tetrahedron formed by the four nearest neighbours. For an ideal tetrahedron, θ is equal to zero. Distributions of the tetrahedricity measure in supercooled water at various densities are shown in figure 1 for $T = 200$ and 300 K. A pronounced two-peak structure of these distributions is visible in the wide density range $0.90 < \rho\ (\mathrm{g\,cm^{-3}}) < 1.40$. The left peak represents water molecules with almost perfect tetrahedral arrangement and it dominates at low densities. The right peak represents water molecules with an essentially isotropic arrangement of neighbours in the first coordination shell. All distributions of θ cross roughly at $0.05 < \theta < 0.06$ at $T = 200$ K, and at slightly larger values of θ at $T = 300$ K. At all studied temperatures, we used the criterion $\theta < 0.06$ to distinguish water molecules with the tetrahedral arrangement of the four nearest neighbours.

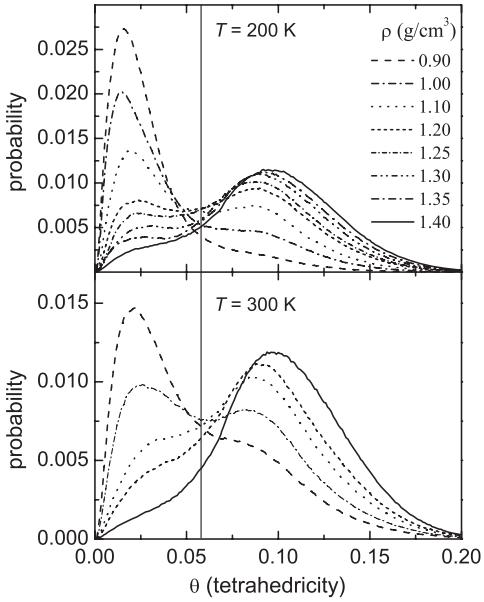

Figure 1. Distribution of the tetrahedricity measure θ (equation (1)) in liquid water of various densities in the one-phase region at $T = 200$ and 300 K.

Percolation analysis was performed for two kinds of water molecules: first, four-coordinated water molecules with tetrahedral arrangement of the nearest neighbours (*four-coordinated* water molecules hereafter); second, water molecules with the tetrahedral arrangement of the four nearest neighbours and any number NN of neighbours in the first coordination shell (*tetrahedrally ordered* water molecules hereafter).

Analysis of water clusters was performed by conventional MC simulations in the NVT ensemble at various densities and temperatures with 512 water molecules in the simulation box. From 1×10^5 to 2×10^5 configurations separated by 1000 MC steps (displacements and rotations) were analysed at each thermodynamic state considered. Percolation transitions were studied at seven temperatures (from $T = 150$ to 290 K) for the four-coordinated water molecules and at five temperatures (from $T = 200$ to 325 K) for the tetrahedrally ordered water molecules. At each studied temperature, the cluster analysis was performed at four to nine average densities. Some of the studied systems were located in liquid–liquid two-phase regions and, therefore, heterogeneous fluctuations may affect clustering properties in the general case. However, we did not see this effect, probably due to the low concentration of the considered species in both coexisting phases.

Two water molecules with the same local order are considered as bonded if one belongs to the first coordination shell of another one. Water molecules belong to the same cluster if they are connected via a continuous path of such bonds. The occurrence frequency of water clusters of various sizes S was described by the cluster size distribution n_S. The mean cluster size was calculated as $S_{\text{mean}} = \Sigma n_S S^2 / \Sigma n_S S$, where the largest cluster was excluded from the sums. $n_S S / \Sigma n_S S$ is a probability that a given water molecule is member of a finite cluster of size S. Each configuration was inspected to detect the presence of an 'infinite' cluster, which spans the periodic cubic simulation box at least in one direction. The probability of observing such a spanning cluster R (spanning probability) was determined at each density studied. We also analysed the probability distribution of the size S_{max} of the largest water cluster and its fractal

dimension. At the percolation threshold in the infinite system, the largest cluster should be a fractal object with a specific fractal dimension d_f. The statistical self-similarity of an infinite fractal leads to the following relationship between its mass $m(r)$ and linear size r:

$$m(r) \sim r^{d_f}. \tag{2}$$

In our analysis of the largest water cluster, $m(r)$ is the number of water molecules in this cluster, which are located inside a sphere of a radius r around a randomly chosen water molecule of the same cluster. The distributions $m(r)$ were averaged over all molecules in the largest cluster. The fractal dimension d_f was determined from the fit of $m(r)$ to equation (2) in the range of r which does not exceed the half of the simulation box.

Various cluster properties show specific behaviour at the percolation threshold. Right at the percolation threshold, the cluster size distribution n_S obeys the universal power law $n_S \sim S^{-\tau}$ [45], with exponents $\tau \approx 2.2$ [46] in the case of 3D random percolation. The mean cluster size S_{mean} diverges at the percolation threshold in an infinite system and passes through a maximum when approaching the threshold in a finite system. Close to the percolation threshold, the probability distribution of the size of the largest cluster is the widest. The fractal dimension of the largest cluster at the percolation threshold is lower than the Euclidean dimension of the system and is equal to $d_f^{3D} \approx 2.53$ for 3D systems [45, 46]. Finally, the spanning probability R is about 50% at the percolation threshold in 3D lattices [47].

3. Results

3.1. Percolation transition of the four-coordinated water molecules

The distribution of tetrahedricity measures θ strongly correlates with the number NN of the water molecules in the first coordination shell [43]. The distributions of tetrahedricity measure for the four-coordinated water molecules at various densities and two temperatures are shown in figure 2. The fraction of the molecules with NN $= 4$ strongly depends on density and temperature. Upon heating of liquid water with $\rho = 0.90$ g cm^{-3} from $T = 200$ to 300 K, it decreases from 67.4% to 40.5%. Increasing density has a more drastic effect: at $T = 200$ K the fraction of molecules with NN $= 4$ is 67.4% and 4.1% at the densities 0.90 and 1.20 g cm^{-3}, respectively. The distribution of the tetrahedricity measure θ for molecules with a certain NN value is not sensitive to the fraction of such molecules (see figure 2 for the case NN $= 4$ and also [43] for other cases). In particular, at $T = 200$ K and $\rho = 0.90$ g cm^{-3} 95% of the water molecules with NN $= 4$ possess a tetrahedral arrangement of the nearest neighbours, whereas at $\rho = 1.20$ g cm^{-3} this fraction is about 91%. Thus, the population of the four-coordinated water molecules considered in the present paper (molecules with NN $= 4$ and $\theta < 0.06$) is only slightly less than the population of molecules with NN $= 4$ and arbitrary values of θ.

The change of the cluster properties of the four-coordinated water molecules with density is qualitatively similar at all studied temperatures. The fraction of these molecules continuously increases with decreasing density and a spanning network of the four-coordinated water molecules at any studied temperature appears at some threshold density value. The spanning probability R shows sigmoid dependence on density, typical for the percolation transition in finite systems (see figure 3). The fit of $R(\rho)$ to the Boltzmann function yields characteristic density ρ_R, where the spanning probability R is about 50%. We estimated $\rho_R = 1.032$ g cm^{-3} at $T = 250$ K. At this density, the fractal dimension of the largest cluster d_f is about 2.02 (figure 4). It achieves the threshold value $d_f^{3D} \approx 2.53$ at essentially lower density $\rho_{3D} \approx 0.99$ g cm^{-3}, where spanning probability R already exceeds 99%.

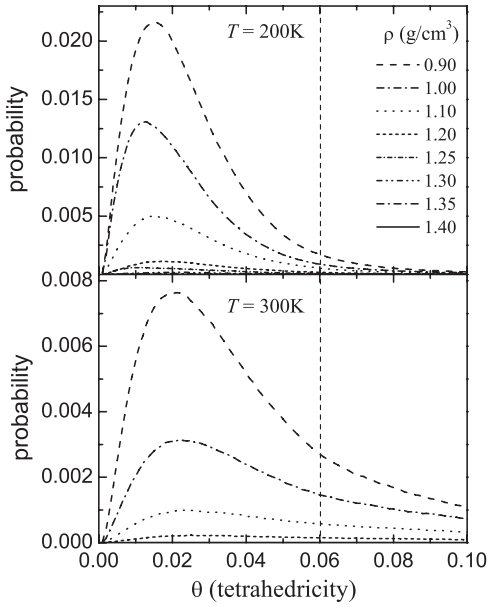

Figure 2. Distribution of the tetrahedricity measure θ (equation (1)) for the four-coordinated molecules in liquid water of various densities in the one-phase region at $T = 200$ and 300 K. The vertical dashed line indicates the chosen criterion $\theta = 0.06$, which distinguishes tetrahedral and non-tetrahedral arrangements of the four nearest neighbours.

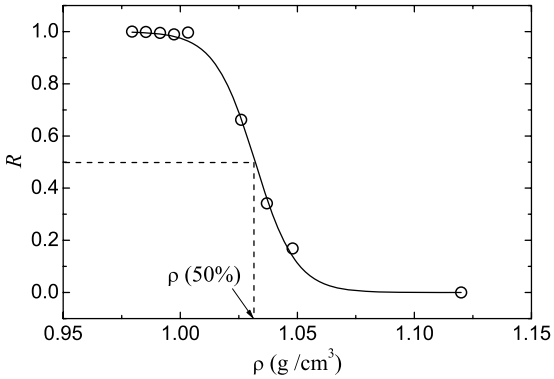

Figure 3. Spanning probability R for the clusters of the four-coordinated water molecules as a function of the average water density at $T = 250$ K. The fit to the Boltzmann function is shown by a solid line. Density ρ_R, where $R \approx 50\%$, is denoted by dashed lines.

The cluster size distributions n_S at $T = 250$ K are shown in figure 5 for several densities. At high water densities, n_S does not follow a power law behaviour shown by solid lines in figure 5. With decreasing density and approaching the percolation threshold, the cluster size distribution becomes closer to the critical power law behaviour $n_S \sim S^{-2.2}$. At $\rho_{3D} \approx 0.99$ g cm^{-3}, n_S follows the critical power law in the widest range of cluster sizes (up to $S \approx 40$). A pronounced hump represents the largest clusters (99% of which are spanning at $\rho_{3D} \approx 0.99$ g cm^{-3}) cut by a finite size of the simulation box. At still lower densities, the negative deviations of n_S from the power law behaviour appear in a wide range of the

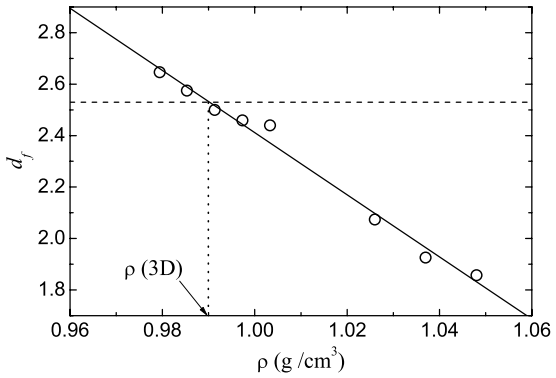

Figure 4. Fractal dimension d_{f} of the largest cluster of the four-coordinated water molecules as a function of the average water density at $T = 250$ K. The linear fit is shown by a solid line. The fractal dimension at the 3D percolation threshold $d_{\mathrm{f}}^{3\mathrm{D}} = 2.53$ is shown by a horizontal dashed line. The location of the percolation threshold $\rho_{3\mathrm{D}}$, where $d_{\mathrm{f}} \approx 2.53$, is denoted by the vertical dotted line.

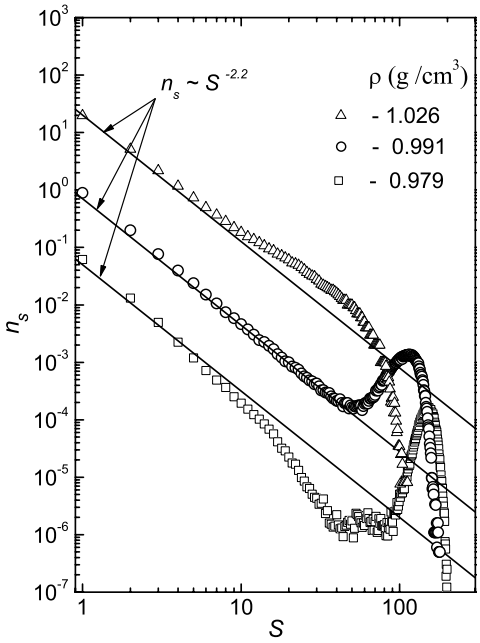

Figure 5. Cluster size distribution n_S of the four-coordinated water molecules at several water densities and $T = 250$ K. The density $\rho = 0.991$ g cm^{-3} is the closest to the percolation threshold. The distributions are shifted consecutively by one order of magnitude each, starting from the bottom.

cluster sizes. The widest probability distribution of the size of the largest cluster is observed at densities close to ρ_R, where the spanning probability is about 50%. The maximum of the mean cluster size S_{mean} is located between ρ_R and $\rho_{3\mathrm{D}}$. The scatter of data for S_{mean} does not allow us to locate its maximum accurately.

The analysis of various clustering properties of the four-coordinated water molecules presented above gives two characteristic values of density at each studied temperature. The

Table 1. Parameters of the percolation thresholds of water molecules with different local orders at various temperatures T: ρ_{3D}, water density; C_{3D}, fraction of water molecules with definite local order; N_{3D}, the average number of water molecules with definite local order in the first coordination shell. The spanning probability R is about 50% at density ρ_R. Temperatures are given in K and densities in g cm^{-3}.

Four-coordinated molecules					Tetrahedrally ordered molecules				
T	ρ_{3D}	C_{3D}	N_{3D}	ρ_R	T	ρ_{3D}	C_{3D}	N_{3D}	ρ_R
150	1.036	0.298	2.04	1.096	200	1.235	0.346	1.80	1.318
200	1.023	0.302	2.04	1.081	235	1.205	0.350	1.75	1.283
250	0.990	0.307	2.05	1.032	275	1.127	0.347	1.75	1.218
260	0.978	0.315	2.06	1.015	300	1.075	0.350	1.75	1.151
270	0.967	0.309	2.05	0.996	325	1.032	0.343	1.75	1.100
280	0.957	0.309	2.08	0.986					
290	0.930	0.312	1.94	—					

percolation threshold is located at $\rho = \rho_{3D}$, when the fractal dimension d_f of the largest clusters achieves the critical value $d_f^{3D} \approx 2.53$ and cluster size distribution n_S obeys the critical power law $n_S \sim S^{-\tau}$ in the widest range of cluster sizes. When $\rho = \rho_R$, the spanning probability is about 50% and the largest clusters show the strongest fluctuations of its size [48–50]. Interestingly, at this density the fractal dimension of the largest cluster is close to 2.0, indicating strongly ramified structure of the largest cluster. The similar two-step formation of the percolating water network is observed in other aqueous systems: aqueous solution [38] and supercritical water [51]. Low fractal dimension of the largest water cluster at ρ_R may reflect specific chain- or sheet-like structure of the spanning water network at mesoscopic scale, which exceeds the size of the simulation box. Formation of such rather large hydrogen-bonded water structures may affect those properties of liquid water which are sensitive to its structure at mesoscopic level. The density ρ_{3D} corresponds to the true percolation threshold, which occurs in an infinitely large system of a size essentially exceeding the characteristic size of the mesoscopic structure of water networks. Namely this threshold has a direct relation to the phase transition.

Two density values, ρ_{3D} and ρ_R, estimated for seven temperatures, are shown in table 1. With increasing temperature from $T = 150$ to 290 K, the threshold density ρ_{3D} moves from $\rho = 1.036$ to 0.93 g cm^{-3}, i.e. it decreases by 10%. Fractions C_{3D} of the four-coordinated water molecules at the percolation threshold are about 30% and practically do not depend on temperature (see table 1). Note that at the percolation threshold the average number N_{3D} of the four-coordinated molecules in the first coordination shell is about 2.05 at all studied temperatures.

3.2. Percolation transition of the tetrahedrally ordered water molecules

The fraction of the molecules with tetrahedral arrangement of the four nearest neighbours and arbitrary number NN of neighbours in the first coordination shell decreases with increasing temperature and density, similarly to the four-coordinated molecules. The fraction of the tetrahedrally ordered molecules at water density $\rho = 0.90$ g cm^{-3} and $T = 200$ K is about 95%. It decreases to 76% upon isochoric heating to 300 K, whereas it decreases to 26% upon isothermic compression to $\rho = 1.30$ g cm^{-3}.

With decreasing density, the spanning probability of the tetrahedrally ordered molecules increases, qualitatively similarly to the case shown in figure 3, that allows estimation of ρ_R (see table 1). The fractal dimension of the largest cluster d_f achieves the critical value $d_f^{3D} = 2.53$

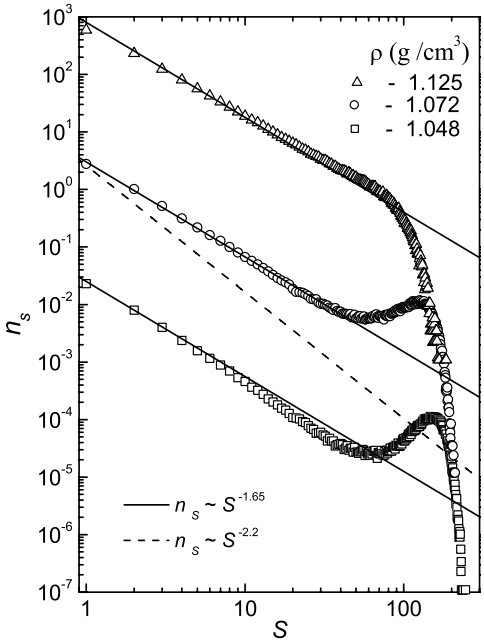

Figure 6. Cluster size distribution n_S of tetrahedrally ordered water molecules at densities close to the percolation threshold at $T = 300$ K. The distributions are shifted vertically by two orders of the magnitude each, starting from the bottom. The power law observed at the percolation threshold $\rho_{3D} = 1.072$ g cm^{-3} is shown by solid lines. The dashed line represents the behaviour of n_S expected at the conventional 3D percolation threshold.

at the threshold density ρ_{3D}, which is noticeably lower than ρ_R. The cluster size distribution n_S shows unusual behaviour close to the percolation threshold (figure 6). When the density is about ρ_{3D}, n_S follows a power law $\sim S^{-\tau}$ in the widest range of cluster sizes S, but with exponent $\tau \approx 1.65$, which is significantly below the value $\tau = 2.2$ for the conventional random 3D percolation.

Density ρ_{3D}, fraction C_{3D} of tetrahedral molecules and number N_{3D} of tetrahedrally ordered neighbours in the first coordination shell at the percolation threshold are shown in table 1 for the five studied temperatures. Similarly to the case of the four-coordinated molecules, the values of C_{3D} and N_{3D} are not sensitive to the temperature and are equal to $\sim$0.35 and 1.75, respectively.

4. Discussion

The line of the percolation transitions of the four-coordinated water molecules is shown in figure 7 together with the liquid–liquid coexistence regions and the liquid branch of the liquid–vapour coexistence curve. Evidently, that percolation transition of the four-coordinated molecules is closely related to the first (lowest density) liquid–liquid phase transition. The line of the percolation transitions is reasonably close to the first liquid–liquid critical point and, probably, to the respective spinodal. To the right from this line the four-coordinated molecules form finite clusters only, whereas at this line an infinite 3D fractal cluster appears. A similar result was obtained when two state points of model TIP4P water with considerably different densities were checked for the presence of the percolating network of four-coordinated molecules [54].

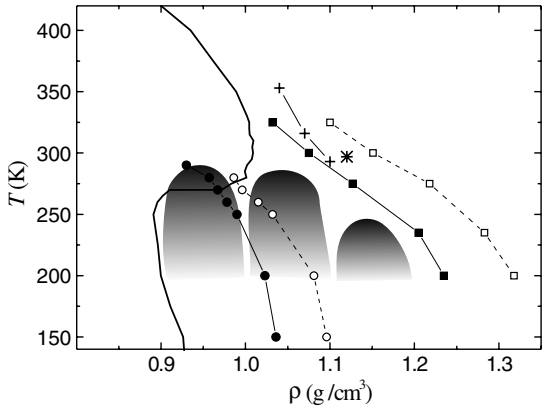

Figure 7. Location of the percolation transitions of the four-coordinated molecules (solid circles) and tetrahedrally ordered molecules (solid squares) with respect to the liquid–liquid coexistence regions (dashed areas) and liquid branch of the liquid–vapour coexistence curve (solid line). The densities ρ_R, where spanning probability $R \approx 50\%$, are shown by respective open symbols. Locations of the anomalies of high-frequency sound velocity observed in [52] and [53] are shown by a star and pluses, respectively.

In the aqueous solution, the immiscibility region approximately corresponds to the concentration interval where both components are above their respective 3D percolation thresholds [38]. As the line of the percolation transitions of the four-coordinated water molecules envelops the coexistence region of the first liquid–liquid transition from the higher density side, we may conclude that the four-coordinated water molecule is the main structural element of the lowest density water phase with $\rho \approx 0.90$ g cm^{-3}. At the percolation threshold the fraction C of the four-coordinated water molecules achieves about 0.3 (see table 1). At higher values of C, system becomes unstable with respect to the phase separation at subcritical temperatures and the lowest density water phase appears via spinodal decomposition. The fraction of the four-coordinated molecules in the stable lowest-density water phase exceeds 0.6 [43].

The line of the percolation transitions of the four-coordinated water molecules crosses the liquid–vapour coexistence curve at the triple point at $T \approx 270$ K, where water vapour coexists with two different liquid phases. The temperatures of the liquid density maximum of real and ST2 water differ by about 35° [16, 17]. So, we may expect that a liquid–liquid–vapour triple point in real water is located at $T \approx 235$ K, i.e. surprisingly close to the homogeneous nucleation temperature T_H. The corresponding spinodal of the first liquid–liquid phase transition [16], as well as the line of the percolation transitions of the four-coordinated water molecules (figure 7), crosses the liquid branch of the liquid–vapour coexistence curve at slightly lower temperature, i.e. close to the temperature where real water shows singular-like behaviour ($T \approx 228$ K [3, 4]). Such a mapping assumes the critical point of the first liquid–liquid transition in real water at $T_C \approx 245$ K and at slightly negative pressure ~ -0.3 kbar. The resulting schematic phase diagram of water in the P–T plane is shown in figure 8.

Among four amorphous phases of ST2 water [16, 17], normal-density water is a phase II, whereas the lowest density phase, an analogue of the LDA, is a phase I [43]. Upon cooling of the normal-density water below the freezing temperature along the liquid–vapour coexistence curve ($P \approx 0$), it remains metastable with respect to crystallization down to the temperature of the liquid–liquid–vapour triple point. At this temperature, phase transition from phase II

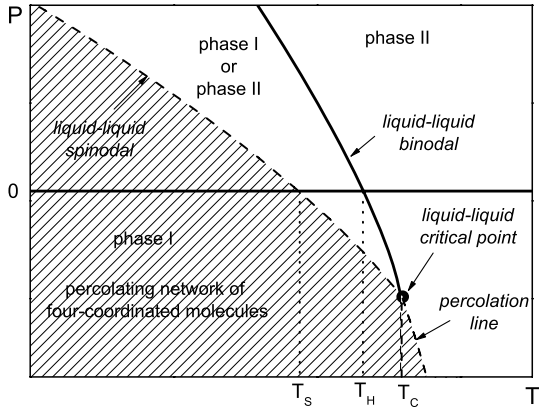

Figure 8. Schematic phase diagram of water. Liquid–vapour ($P \approx 0$) and liquid–liquid binodals are shown by solid lines. The line of the percolation transitions of the four-coordinated molecules and the liquid–liquid spinodal are shown by dashed lines. Characteristic temperatures T_S, T_H and T_C are indicated by vertical lines. In the region between the liquid–liquid binodal and spinodal, a percolation network of the four-coordinated molecules exists in phase I.

to phase I occurs. In contrast to phase II, phase I has an analogue among the crystalline ices (hexagonal ice) with similar structure and density. Therefore, we may suppose that phase I becomes unstable with respect to crystallization at higher temperatures, then phase II. In such a case, the homogeneous nucleation of water should occur immediately after the phase transition from phase II to phase I, i.e. at $T = T_H$ (figure 8).

A singular-like behaviour of real water on approaching the temperature $T_S \approx 228$ K reflects approaching the spinodal of the first liquid–liquid transition, which in fact coincides with (or is very close to) the line of the percolation transitions of the four-coordinated molecules. So, the explanation of the anomalous properties of water, based on the percolation transition, is intrinsically the same as their explanation based on the liquid–liquid transition. This conclusion also remains valid when the first liquid–liquid phase transition ends at the critical point at positive pressures (this is the case for the ST water model with long-range corrections for Coulombic interaction [25, 16, 17, 26]). The line of the percolation transitions, which starts from such a critical point, ultimately crosses the liquid–vapour coexistence curve at a certain temperature. Formation of an infinite network of the four coordinated water molecules (via crossing the liquid–liquid transition or via crossing the percolation line at supercritical temperatures) may strongly affect various water properties, including its dynamics [55, 56]. Note that in water models with weaker tetrahedral structure (in some implementations of TIP4P model or in the SPCE model) the water phase of density $\rho \approx 0.90$ g cm^{-3} exists at strongly negative pressures only [17], and percolation transition of the four-coordinated molecules may not affect the properties of the saturated liquid at $P \approx 0$.

The density threshold values ρ_R for the four-coordinated water molecules are shown in figure 7 by open circles. At these densities, the largest clusters (patches) of the four-coordinated water molecules contain several dozen water molecules each and their sizes become comparable with the size of the simulation box (∼25 Å). The appearance of such extended networks of the four-coordinated water molecules may affect some properties of liquid water, which are sensitive to the structure on a mesoscopic scale. In particular, development of such mesoscopic structures may be responsible for the specific increase of the water density fluctuations measured by x-ray scattering in a certain temperature range [57, 58].

The obtained line of the percolation transitions of molecules with tetrahedral local order envelops the whole region where liquid–liquid immiscibility occurs (figure 7). This demonstrates the crucial role of the tetrahedral arrangement in all liquid–liquid transitions. There is no infinite network of tetrahedrally ordered water molecules to the right of this percolation line. The absence of such a network is a characteristic feature of the highest density water phase, which consists mainly of molecules with highly isotropic angular distribution of nearest neighbours and has structure similar to the structure of VHDA [43]. Contrary to the percolation of the four-coordinated water molecules, the cluster size distribution of the tetrahedrally ordered water molecules at the percolation threshold follows a power law with a non-universal value of the critical exponent $\tau \approx 1.65$. The latter value appears in systems with an intrinsic disorder [59]. In our case, disorder may originate from the rather ambiguous definition of the local order responsible for the highest density liquid–liquid phase transition. Alternatively, this disorder may be an intrinsic property of a liquid–liquid phase transition in one-component isotropic fluids.

Formation of spanning network of tetrahedrally ordered molecules may affect properties of liquid water at high densities. In fact, an anomaly in the high-frequency sound velocity is observed experimentally at ambient temperature, when the density is slightly larger than 1.1 g cm^{-3} [52, 53]. The locations of the thermodynamic points where such an anomaly was observed are close to the line of percolation transition of tetrahedrally ordered water molecules seen in simulations (see figure 7).

Acknowledgment

Financial support from Deutsche Forschungsgemeinschaft (DFG 486) is gratefully acknowledged.

References

[1] Chadwell H M 1927 *Chem. Rev.* **4** 357
[2] Whiting H 1884 *A Theory of Cohesion* vol 70 (Cambridge: Harvard University Press)
[3] Anisimov M A, Voronel A V, Zaugolnikova N S and Ovodov G I 1972 *JETP Lett.* **15** 317
[4] Angell C A, Shuppert J and Tucker J C 1973 *J. Phys. Chem.* **77** 3092
[5] Stanley H E 1979 *J. Phys. A: Math. Gen.* **12** L329
[6] Stanley H E and Teixeira J 1980 *J. Chem. Phys.* **73** 3404
[7] Stanley H E and Teixeira J 1980 *Ferroelectrics* **30** 213
[8] Geiger A, Stillinger F H and Rahman A 1979 *J. Chem. Phys.* **70** 4185
[9] Stanley H E, Teixeira J, Geiger A and Blumberg R L 1981 *Physica* A **106** 260
[10] Geiger A and Stanley H E 1982 *Phys. Rev. Lett.* **49** 1749
[11] Blumberg R L, Stanley H E, Geiger A and Mausbach P 1984 *J. Chem. Phys.* **80** 5230
[12] Geiger A and Stanley H E 1982 *Phys. Rev. Lett.* **49** 1895
[13] Mishima O, Calvert L D and Whalley E 1985 *Nature* **314** 76
[14] Debenedetti P G 2003 *J. Phys.: Condens. Matter* **15** R1669
[15] Loerting T, Salzmann C, Kohl I, Mayer E and Hallbrucker A 2001 *Phys. Chem. Chem. Phys.* **3** 5355
[16] Brovchenko I, Geiger A and Oleinikova A 2003 *J. Chem. Phys.* **118** 9473
[17] Brovchenko I, Geiger A and Oleinikova A 2005 *J. Chem. Phys.* **123** 044515
[18] Jedlovszky P and and Vallauri R 2005 *J. Chem. Phys.* **122** 081101
[19] Loerting T, Schustereder W, Winkel K, Salzmann C G, Kohl I and Mayer E 2006 *Phys. Rev. Lett.* **96** 025702
[20] Poole P H, Sciortino F, Grande T, Stanley H E and Angell C A 1994 *Phys. Rev. Lett.* **73** 1632
[21] Borick S S, Debenedetti P G and Sastry S 1995 *J. Phys. Chem.* **99** 3781
[22] Tanaka H 1996 *J. Chem. Phys.* **105** 5099
[23] Truskett T M, Debenedetti P G, Sastry S and Torquato S 1999 *J. Chem. Phys.* **111** 2647
[24] Franzese G, Marques M I and Stanley H E 2003 *Phys. Rev.* E **67** 011103

[25] Poole P H, Sciortino F, Essmann U and Stanley H E 1992 *Nature* **360** 324
[26] Xu L, Kumar P, Buldyrev S V, Chen S H, Poole P H, Sciortino F and Stanley H E 2005 *Proc. Natl Acad. Sci.* **102** 16558
[27] Roberts C J and Debenedetti P G 1996 *J. Chem. Phys.* **105** 658
[28] Poole P H, Saika-Voivod I and Sciortino F 2005 *J. Phys.: Condens. Matter* **17** L431
[29] Sastry S, Debenedetti P G, Sciortino F and Stanley H E 1996 *Phys. Rev.* E **53** 6144
[30] Narayan T and Kumar A 1994 *Phys. Rep.* **249** 135
[31] Schneider G M 2002 *Phys. Chem. Chem. Phys.* **4** 845
[32] Visak Z P, Rebelo L P N and Szydlowski J 2003 *J. Phys. Chem.* B **107** 9837
[33] Sorensen C M and Larsen G A 1985 *J. Chem. Phys.* **83** 1835
[34] Franzese G, Malescio G, Skibinsky A, Buldyrev S V and Stanley H E 2001 *Nature* **409** 692
[35] Franzese G, Malescio G, Skibinsky A, Buldyrev S V and Stanley H E 2002 *Phys. Rev.* E **66** 051206
[36] Coniglio A and Klein W 1980 *J. Phys. A: Math. Gen.* **13** 2775
[37] Klein W 1981 *Phys. Rev. Lett.* **47** 1569
[38] Oleinikova A, Brovchenko I, Geiger A and Guillot B 2002 *J. Chem. Phys.* **117** 3296
[39] Stillinger F H and Rahman A 1974 *J. Chem. Phys.* **60** 1545
[40] Panagiotopoulos A Z 1987 *Mol. Phys.* **61** 813
[41] Hansen J P and Verlet L 1969 *Phys. Rev.* **184** 151
[42] Corti D S and Debenedetti P G 1994 *Chem. Eng. Sci.* **49** 2717
[43] Brovchenko I and Oleinikova A 2006 *J. Chem. Phys.* at press
[44] Naberukhin Yu I, Voloshin V P and Medvedev N N 1991 *Mol. Phys.* **73** 917
[45] Stauffer D 1985 *Introduction to Percolation Theory* (London: Taylor and Francis)
[46] Jan N 1999 *Physica* A **266** 72
[47] Martins P H L and Plascak J A 2003 *Phys. Rev.* E **67** 046119
[48] Brovchenko I and Oleinikova A 2006 *Handbook of Theoretical and Computational Nanotechnology* ed M Rieth and W Schommers (Stevenson Ranch, CA: American Scientific Publishers)
[49] Oleinikova A, Smolin N, Brovchenko I, Geiger A and Winter R 2005 *J. Phys. Chem.* B **109** 1988
[50] Oleinikova A, Brovchenko I, Smolin N, Krukau A, Geiger A and Winter R 2005 *Phys. Rev. Lett.* **95** 247802
[51] Partay L, Jedlovszky P, Brovchenko I and Oleinikova A 2006 *Phys. Rev. Lett.* submitted
[52] Krisch M, Loubeyre P, Ruocco G, Sette F, D'Astuto M, LeToulec R, Lorenzen M, Mermet A, Monaco G and Verbeni R 2002 *Phys. Rev. Lett.* **89** 125502
[53] Li F, Cui Q, He Z, Cui T, Zhang J, Zhou Q, Zou G and Sasaki S 2005 *J. Chem. Phys.* **123** 174511
[54] Tanaka H 1998 *Phys. Rev. Lett.* **80** 113
[55] Faraone A, Liu L, Mou C Y, Yen C W and Chen S H 2004 *J. Chem. Phys.* **121** 10843
[56] Liu L, Chen S H, Faraone A, Yen C W and Mou C Y 2005 *Phys. Rev. Lett.* **95** 117802
[57] Bosio L, Teixeira J and Stanley H E 1981 *Phys. Rev. Lett.* **46** 597
[58] Xie Y, Ludwig K F Jr, Morales G, Hare D E and Sorensen C M 1993 *Phys. Rev. Lett.* **71** 2050
[59] Dahmen K and Sethna J P 1996 *Phys. Rev.* B **53** 14872